Inorganic Chemistry

Article

pubs.acs.org/IC

Oxygen Reduction Reactions of Monometallic Rhodium Hydride Complexes

Thomas S. Teets and Daniel G. Nocera*

Department of Chemistry, 6-335, Massachusetts Institute of Technology, 77 Massachusetts Avenue, Cambridge, Massachusetts 02139-4307, United States

Supporting Information

ABSTRACT: Selective reduction of oxygen is mediated by a series of monometallic rhodium(III) hydride complexes. Oxidative addition of HCl to *trans*-$Rh^{I}Cl(L)(PEt_3)_2$ (**1a**, L = CO; **1b**, L = 2,6-dimethylphenylisocyanide (CNXy); **1c**, L = 1-adamantylisocyanide (CNAd)) produces the corresponding Rh^{III} hydride complex *cis-trans*-$Rh^{III}Cl_2H(L)(PEt_3)_2$ (**2a**–**c**). The measured equilibrium constants for the HCl-addition reactions show a pronounced dependence on the identity of the "L" ligand. The hydride complexes effect the reduction of O_2 to water in the presence of HCl, generating *trans*-$Rh^{III}Cl_3(L)(PEt_3)_2$ (**3a**–**c**) as the metal-containing product. In the case of **2a**, smooth conversion to **3a** proceeds without spectroscopic evidence for an intermediate species. For **2b**/**c**, an aqua intermediate, *cis-trans*-$[Rh^{III}(OH_2)Cl_2(L)(PEt_3)_2]Cl$ (**5b**/**c**), forms along the pathway to producing **3b**/**c** as the final products. The aqua complexes were independently prepared by treating peroxo complexes *trans*-$Rh^{III}Cl(L)(\eta^2\text{-}O_2)(PEt_3)_2$ (**4b**/**c**) with HCl to rapidly produce a mixture of **5b**/**c** and **3b**/**c**. The reactivity of the peroxo species demonstrates that they are plausible intermediates in the O_2-reduction chemistry of hydride complexes **2a**–**c**. These results together show that monometallic rhodium hydride complexes are capable of promoting selective reduction of oxygen to water and that this reaction may be controlled with systematic alteration of the ancillary ligand set.

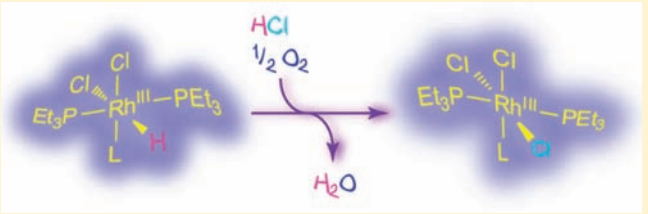

INTRODUCTION

The fundamental reactivity of O_2 at transition metal centers is at the nexus of bioenergy[1,2] and chemical energy[3,4] conversion. In nature, oxidase[5] and oxygenase[6,7] enzymes utilize O_2 as the oxidant in crucial respiratory and biosynthetic catalyses by managing both the proton and electron inventory. With an eye toward designing biomimetic catalysts and gaining a more thorough understanding of energy-conversion mechanisms, numerous model complexes designed to retain key features of the enzyme active sites have appeared.[8−10] By appending either Brønsted acids[11,12] or auxiliary metal centers[9,13−17] in the secondary coordination sphere of a metallomacrocycle, biofunctional O_2 reduction catalysts have been realized. In addition, because of oxygen's abundance and environmental compatibility, in the realm of synthetic chemistry there is considerable appeal in developing catalytic systems that utilize O_2 as the sole oxidizing species.[18,19] Complexes of iron,[20] copper,[21] rhodium,[22] and select other metals[23−25] can catalyze aerobic oxidation reactions, though palladium catalysis is the most widespread.[18,26−28]

Insertion of O_2 into metal−hydride bonds often plays a key role in its activation, especially if the reactions occur in acidic media and/or are attendant to C−H activation. As such, in-depth studies of the reactions of O_2 with metal hydride complexes are germane to numerous topics in catalysis. There are many examples of O_2 insertion into metal hydrides to furnish hydroperoxo complexes,[29−41] and in recent years mechanistic studies of the aerobic oxidation of group 10 metal hydrides and especially those involving palladium have proliferated in the context of the aerobic oxidation catalysis.[42−48] Mechanistic studies of O_2 reactivity with group 9 metal hydrides were less numerous[32,35,41] leading up to our observation that dirhodium hydride complexes, accessed by reversible HCl addition to two-electron mixed-valent centers, promote the reduction of oxygen to water.[49] The analogous diiridium hydride complex inserts O_2 to form an isolable hydroperoxo complex.[50] This finding, coupled with kinetic[51] and computational analyses[52] of both the dirhodium and the diiridium systems, led us to conclude that a hydroperoxo complex is a key intermediate in the $4e^-/4H^+$ oxygen reduction reaction (ORR) of O_2 to water. Though select examples involve radical chain mechanisms,[32,53] most of these recent mechanistic studies reveal two common pathways for insertion of O_2 into a metal−hydride bond: (i) the "HX reductive elimination" (HXRE) mechanism,[41,45,48] where reductive elimination precedes reaction of the reduced metal center with O_2, and (ii) "H-atom abstraction" (HAA),[42] where O_2 reacts directly with the metal hydride. It has been observed experimentally that it is possible in some systems for these two mechanisms to be competitive and occur simultaneously.[46,51,52]

The proclivity of the HXRE and HAA mechanisms to compete in the ORR offers the opportunity to assess the electronic factors that are determinants of the HXRE and HAA

Received: February 7, 2012
Published: June 18, 2012

   dx.doi.org/10.1021/ic300279z | *Inorg. Chem.* 2012, 51, 7192−7201

pathways and thus provide further insight into the preferred mechanism(s) of the aerobic oxidation reactions. We sought to tune the reactivity of the metal center by systematic alteration of the electronic properties of the ligand set of the metal center. In this regard, the two-electron mixed-valent dirhodium and diiridium complexes that served as the starting points for our previous studies[49,51] offer few synthetic inroads to tune the electronic properties of these scaffolds. Such a line of inquiry thus demands the construction of new transition metal scaffolds to effect ORR activity. We also sought to better understand the role of the second metal in the O_2 activation chemistry of bimetallic centers and whether metal cooperativity at two-electron mixed-valent centers[54] offered any benefits for the ORR. Accordingly, we set out to interrogate O_2 activation and reduction at monometallic rhodium hydride complexes. Our findings are disclosed herein.

Three isostructural rhodium hydride complexes of the type *cis-trans*-$Rh^{III}Cl_2H(L)(PEt_3)_2$ (where L = CO, 2,6-dimethylphenylisocyanide (CNXy), or 1-adamantylisocyanide (CNAd)) are found to promote the ORR cleanly in the presence of HCl with the attendant production of the corresponding *trans*-$Rh^{III}Cl_3(L)(PEt_3)_2$. Alteration of L has a dramatic effect on both the HCl-addition equilibrium constant and the O_2-binding thermodynamics of the parent Rh^I complexes. We show that when L is an isocyanide, an aqua–rhodium(III) intermediate forms prior to generation of the final product. By interrogating the reactivity of the O_2 adducts *trans*-$Rh^{III}Cl(CNR)(\eta^2\text{-}O_2)(PEt_3)_2$ (R = 2,6-dimethylphenyl, 1-adamantyl) we also demonstrate that these η^2-peroxo complexes and the spectroscopically unobserved hydroperoxo complexes are plausible intermediates in the ORR of the hydride complexes.

EXPERIMENTAL SECTION

General Considerations. All reactions involving air-sensitive materials were executed in a N_2-filled glovebox, on a Schlenk line, or on a high-vacuum manifold using solvents previously dried by passage through an alumina column under Ar. HCl (4 M in dioxane, 1 M in Et_2O), anhydrous NaCl, concentrated H_2SO_4, anhydrous 1,4-dioxane, and 2,6-dimethylphenylisocyanide (CNXy) were obtained from Sigma-Aldrich, $[Rh^I(CO)_2Cl]_2$, $[Rh^ICl(COD)]_2$ (COD = 1,5-cyclooctadiene), and PEt_3 were purchased from Strem, and O_2 was purchased from Airgas. All commercially available starting materials were used as received. The complex *trans*-$Rh^ICl(CO)(PEt_3)_2$ (**1a**) was prepared by a modified procedure,[55] starting with $[Rh^I(CO)_2Cl]_2$ and using toluene as the solvent. The ligand 1-adamantylisocyanide (CNAd) was prepared as described previously.[56] Elemental analyses were performed by Midwest Microlab LLC.

Physical Methods. NMR spectra were recorded at the MIT Department of Chemistry Instrumentation Facility on Varian Mercury-300 or Inova-500 NMR spectrometers. $^{31}P\{^1H\}$ NMR spectra were referenced to an external standard of 85% D_3PO_4, and ^1H spectra were referenced to the residual proteo solvent resonances. UV–vis spectra were recorded at 295 K in THF solutions in quartz cuvettes on a Varian Cary 5000 UV–vis–NIR spectrophotometer. Extinction coefficients were determined over a concentration range from $\sim10^{-6}$ to 10^{-4} M, for which all compounds obeyed Beer's Law. For hydride complexes **2b/c**, UV–vis spectra were recorded in the presence of 52 mM HCl, whereas for **4b/4c**, spectra were recorded with 1 atm of O_2 present to prevent reversion to **1b/c**. Spectral data is summarized below, and full electronic spectra are presented in the Supporting Information, Figures S4–S13. IR spectra were recorded on a PerkinElmer Spectrum 400 FT-IR/FT-FIR spectrometer outfitted with a Pike Technologies GladiATR attenuated total reflectance accessory with a monolithic diamond crystal stage and pressure clamp. Samples were suspended in Nujol for all IR measurements.

Preparation of *trans*-$Rh^ICl(CNXy)(PEt_3)_2$ (1b). In a 20 mL scintillation vial, $[Rh^I(COD)Cl]_2$ (100 mg, 0.203 mmol, 1.00 equiv) was suspended in 2 mL of THF. A solution of PEt_3 (120 μL, 0.811 mmol, 4.00 equiv) dissolved in 2 mL of THF was added, producing a light orange solution. Immediate addition of 2,6-dimethylphenylisocyanide (CNXy) (53 mg, 0.40 mmol, 2.0 equiv) in 2 mL of THF caused the color to fade to bright yellow. The slightly cloudy mixture was stirred for 1 h at room temperature and then filtered to remove a small amount of gray solid. The resulting yellow solution was concentrated in vacuo to give a sticky yellow solid, which was redissolved in 8 mL of hexane. The solvent was removed in vacuo, and the resulting microcrystalline yellow solid was dried in vacuo overnight to remove residual 1,5-cyclooctadiene. Yield: 200 mg (97.6%). ^1H NMR (500 MHz, C_6D_6) δ/ppm: 6.76–6.82 (m, 3H), 2.33 (s, 6H), 1.80 (m, 12H) 1.11 (quintet, 18H). $^{31}P\{^1H\}$ NMR (121.5 MHz, C_6D_6) δ/ppm: 23.6 (d, $^1J_{Rh-P}$ = 124 Hz). UV–vis (THF): λ/nm (ε/M^{-1} cm^{-1}) 265 (24 000), 302 (sh) (8100), 367 (sh) (2600). IR (Nujol): $\tilde{\nu}_{C\equiv N}$ = 2054 cm^{-1}. Anal. Calcd for $C_{21}H_{39}ClNP_2Rh$: C, 49.86; H, 7.77; N, 2.77. Found: C, 49.59; H, 7.69; N, 2.64.

Preparation of *trans*-$Rh^I(CNAd)Cl(PEt_3)_2$ (1c). THF solutions (2 mL) of $[Rh^I(COD)Cl]_2$ (100 mg, 0.203 mmol, 1.00 equiv) and PEt_3 (120 μL, 0.811 mmol, 4.00 equiv) were combined to afford a pale orange solution. 1-Adamantylisocyanide (CNAd) (66 mg, 0.41 mmol, 2.0 equiv) in 2 mL of THF was introduced, causing the color to fade to yellow. After stirring for 1 h at room temperature, the solution was concentrated in vacuo to leave a yellow residue, which was redissolved in 4 mL of pentane. The yellow solution was concentrated and dried in vacuo overnight, leaving the product as a bright yellow solid. Yield: 208 mg (95.8%). ^1H NMR (500 MHz, C_6D_6) δ/ppm: 1.88 (m, 12H), 1.80 (br, d, 6H), 1.73 (br, m, 3H), 1.33 (br, m, 6H), 1.20 (quintet, 18H). $^{31}P\{^1H\}$ NMR (121.5 MHz, C_6D_6) δ/ppm: 22.8 (d, $^1J_{Rh-P}$ = 127 Hz). UV–vis (THF): λ/nm (ε/M^{-1} cm^{-1}) 282 (sh) (5700), 308 (9700), 369 (3900). IR (Nujol): $\tilde{\nu}_{C\equiv N}$ = 2068 cm^{-1}. Anal. Calcd for $C_{23}H_{45}ClNP_2Rh$: C, 51.55; H, 8.46; N, 2.61. Found: C, 51.42; H, 8.15; N, 2.53.

Preparation and NMR Characterization of *cis-trans*-$Rh^{III}(CO)Cl_2H(PEt_3)_2$ (2a). A J. Young NMR tube was charged with **1a** (10 mg, 0.025 mmol) dissolved in 0.7 mL of THF-d_8. The solution was freeze–pump–thaw degassed three times at $\sim10^{-6}$ Torr on a high-vacuum manifold. Anhydrous HCl, generated by dropping concentrated H_2SO_4 onto anhydrous NaCl (36 mg, 0.62 mmol, 25 equiv), was vacuum transferred to the solution of **1a**. While frozen, the NMR tube was evacuated to $\sim10^{-6}$ Torr and then thawed to reveal a pale yellow solution. Under these conditions (where HCl transfer is not quantitative), **2a** and **1a** were observed to be present in a ca. 2:1 ratio. Removal of the volatiles resulted in complete reversion to **1a**, as judged by $^{31}P\{^1H\}$ NMR. ^1H NMR (500 MHz, THF-d_8) δ/ppm: 2.10 (m, 12H), 1.18 (quintet, 18H), −13.16 (dt, $^1J_{Rh-H}$ = 16.6 Hz, $^2J_{P-H}$ = 10.4 Hz, 1H). $^{31}P\{^1H\}$ NMR (121.5 MHz, THF-d_8) δ/ppm: 26.4 (d, $^1J_{Rh-P}$ = 81 Hz).

Preparation of *cis-trans*-$Rh^{III}Cl_2(CNXy)H(PEt_3)_2$ (2b). A 25 mL Schlenk tube with a Teflon plug seal was charged with **1b** (100 mg, 0.198 mmol) dissolved in 3 mL of THF. The solution was freeze–pump–thaw degassed three times at $\sim10^{-6}$ Torr. Anhydrous HCl, generated by dropping concentrated H_2SO_4 onto anhydrous NaCl (58 mg, 0.99 mmol, 5.0 equiv), was vacuum transferred onto the still-frozen solution. The vessel was pumped down to $\sim10^{-6}$ Torr and then allowed to thaw slowly with stirring. Upon thawing, the now colorless solution was stirred for 10 min. The volatiles were removed in vacuo, and the resulting residue was taken back into the glovebox, dissolved in 4 mL of THF, and transferred to a scintillation vial. Solvent was removed in vacuo to yield a pale residue, which was suspended in 0.25 mL of toluene. Addition of 4 mL of hexane separated a white solid, which was decanted and dried in vacuo. Yield: 100 mg (93.4%). ^1H NMR (500 MHz, C_6D_6) δ/ppm: 6.74 (t, $^3J_{H-H}$ = 7.6 Hz, 1H), 6.64 (d, $^3J_{H-H}$ = 7.6 Hz, 2H), 2.29 (s, 6H), 2.08 (m, 6H), 1.90 (m, 6H), 1.05, (quintet, 18H), −14.48 (dt, $^1J_{Rh-H}$ = 18.1 Hz, $^2J_{P-H}$ = 11.4 Hz, 1H). $^{31}P\{^1H\}$ NMR (121.5 MHz, C_6D_6) δ/ppm: 24.7 (d, $^1J_{Rh-P}$ = 86 Hz). UV–vis (THF): λ/nm (ε/M^{-1} cm^{-1}) 251 (27 000). IR (Nujol): $\tilde{\nu}_{C\equiv N}$

dx.doi.org/10.1021/ic300279z | Inorg. Chem. 2012, 51, 7192–7201

= 2147 cm^{-1}. Anal. Calcd for $C_{21}H_{40}Cl_2NP_2Rh$: C, 46.51; H, 7.43; N, 2.58. Found: C, 46.29; H, 7.27; N, 2.41.

Preparation of *cis-trans*-Rh^{III}(CNAd)$Cl_2H(PEt_3)_2$ (2c). A 25 mL Schlenk flask was charged with **1c** (100 mg, 0.186 mmol) dissolved in 6 mL of Et_2O. After cooling to −78 °C in dry ice/acetone, a solution of HCl in Et_2O (1.03 M, 0.90 mL, 5.0 equiv) was added via syringe. The reaction mixture was stirred for 10 min before removing the cold bath. A white precipitate that formed initially redissolved upon warming to room temperature, yielding a colorless solution that was stirred for 30 min. The solution was concentrated in vacuo to give a white solid. In the glovebox, the solid was suspended in 8 mL of Et_2O and transferred to a scintillation vial. Solvent was removed in vacuo, and the solid was redissolved in 0.5 mL of toluene. With stirring, 6 mL of hexane was added, freeing a colorless solid, which was decanted and dried in vacuo. Yield: 97 mg (91%). ^{1}H NMR (500 MHz, C_6D_6) δ/ppm: 2.14 (m, 6H), 1.98 (m, 6H), 1.65 (br, d, 6H), 1.61 (br, m, 3H), 1.17−1.27 (br, m, 6H), 1.15, (quintet, 18H), −15.09 (dt, $^1J_{Rh-H}$ = 17.9 Hz, $^2J_{P-H}$ = 11.6 Hz, 1H). $^{31}P\{^1H\}$ NMR (121.5 MHz, C_6D_6) δ/ppm: 24.1 (d, $^1J_{Rh-P}$ = 88 Hz). UV−vis (THF): λ/nm (ε/M^{-1} cm^{-1}) 233 (sh) (14 000), 277 (7200). IR (Nujol): $\tilde{\nu}_{C\equiv N}$ = 2170 cm^{-1}. Anal. Calcd for $C_{23}H_{46}Cl_2NP_2Rh$: C, 48.26; H, 8.10; N, 2.45. Found: C, 48.33; H, 7.81; N, 2.32.

Preparation of *trans*-Rh^{III}(CO)$Cl_3(PEt_3)_2$ (3a). In a 20 mL scintillation vial, **1a** (50 mg, 0.12 mmol) was dissolved in 1 mL of CH_2Cl_2. Separately, $PhICl_2$ (28.5 mg, 0.104 mmol, 1.05 equiv) was also dissolved in 1 mL of CH_2Cl_2. Both solutions were frozen in the coldwell of the glovebox. They were removed, and upon thawing the $PhICl_2$ was added dropwise to the stirred solution of **1a**, giving a bright yellow solution which was allowed to warm to room temperature and stirred for 30 min. At this time, 4 mL of hexane was added, and the solution was concentrated in vacuo to produce a sticky yellow solid. Washing the product with 2 mL of hexane at −20 °C gave a yellow solid, which was dried in vacuo. The spectral data reported here are a good match for those reported previously.[57,58] Yield: 55 mg (93%). ^{1}H NMR (500 MHz, C_6D_6) δ/ppm: 2.02 (M, 12H), 0.98 (quintet, 18H). $^{31}P\{^1H\}$ NMR (121.5 MHz, C_6D_6) δ/ppm: 19.3 (d, $^1J_{Rh-P}$ = 72 Hz). UV−vis (THF): λ/nm (ε/M^{-1} cm^{-1}) 295 (20 000), 371 (2000). IR (Nujol): $\tilde{\nu}_{C\equiv O}$ = 2059 cm^{-1}. Anal. Calcd for $C_{13}H_{30}Cl_3OP_2Rh$: C, 32.97; H, 6.38. Found: C, 32.48; H, 6.16.

Preparation of *trans*-$Rh^{III}Cl_3$(CNXy)$(PEt_3)_2$ (3b). A sample of **1b** (50 mg, 0.099 mmol) was dissolved in 1 mL of toluene. In a separate vial, $PhICl_2$ (28.5 mg, 0.104 mmol, 1.05 equiv) was also dissolved in 1 mL of toluene. Both solutions were frozen in the coldwell of the glovebox. They were removed, and upon thawing the $PhICl_2$ was added dropwise to the stirred solution of **1b** with a slight darkening in color observed. The solution was allowed to warm to room temperature and stirred for a total of 40 min. At this time, the solvent was removed in vacuo to leave a yellow-orange residue, which was redissolved in 0.5 mL of CH_2Cl_2. With stirring, 3 mL of hexane was added, and the mixture was concentrated to ca. one-half its original volume, liberating a yellow-orange solid. The supernatant was decanted, and the product was dried in vacuo. The solid was redissolved in 2 mL of toluene, and after sitting for 4 days at room temperature complete conversion from a mixture of *trans*-$Rh^{III}Cl_3$(CNXy)$(PEt_3)_2$ and *mer-cis*-$Rh^{III}Cl_3$(CNXy)$(PEt_3)_2$ to the desired trans product was achieved. Toluene was removed in vacuo to reveal a yellow solid, which was dissolved in a mixture of 0.5 mL of CH_2Cl_2 and 4 mL of hexane. After concentrating in vacuo to <2 mL, the supernatant was separated from the yellow-orange product, which was dried in vacuo. Yield: 46 mg (81%). ^{1}H NMR (500 MHz, C_6D_6) δ/ppm: 6.73 (t, $^3J_{H-H}$ = 7.6 Hz, 1H), 6.63 (d, $^3J_{H-H}$ = 7.6 Hz, 2H), 2.37 (s, 6H), 2.18 (m, 12H), 1.09 (quintet, 18H). $^{31}P\{^1H\}$ NMR (121.5 MHz, C_6D_6) δ/ppm: 15.4 (d, $^1J_{Rh-P}$ = 77 Hz). UV−vis (THF): λ/nm (ε/M^{-1} cm^{-1}) 254 (37 000), 345 (2800), 398 (sh) (920). IR (Nujol): $\tilde{\nu}_{C\equiv N}$ = 2190 cm^{-1}. Anal. Calcd for $C_{21}H_{39}Cl_3NP_2Rh$: C, 43.73; H, 6.82; N, 2.43. Found: C, 43.44; H, 6.50; N, 2.31.

Preparation of *trans*-Rh^{III}(CNAd)$Cl_3(PEt_3)_2$ (3c). A 20 mL scintillation vial was charged with **1c** (50 mg, 0.093 mmol), and into a separate vial was weighed $PhICl_2$ (27 mg, 0.098 mmol, 1.05 equiv). Both solids were dissolved in 1 mL of CH_2Cl_2 and frozen in the glovebox coldwell. They were removed, and upon thawing the $PhICl_2$ solution was added dropwise to the **1c** solution, yielding a bright yellow-orange solution which was warmed to room temperature and stirred for 30 min. The solution was diluted with 4 mL of hexane and concentrated in vacuo to afford a yellow-orange residue. The residue was taken up in 0.25 mL of CH_2Cl_2, to which was added 4 mL of hexane to produce a cloudy mixture. Upon concentrating in vacuo to <2 mL, a yellow-orange solid precipitated. The supernatant was decanted, and the product was dried in vacuo. Yield: 53 mg (93%). ^{1}H NMR (500 MHz, C_6D_6) δ/ppm: 2.25 (m, 12H), 1.72 (br, d, 6H), 1.61 (br, m, 3H), 1.13−1.25 (m, 24H). $^{31}P\{^1H\}$ NMR (121.5 MHz, C_6D_6) δ/ppm: 14.4 (d, $^1J_{Rh-P}$ = 78 Hz). UV−vis (THF): λ/nm (ε/M^{-1} cm^{-1}) 222 (25 000), 262 (15 000), 272 (sh) (14 000), 341 (2100), 403 (560). IR (Nujol): $\tilde{\nu}_{C\equiv N}$ = 2194 cm^{-1}. Anal. Calcd for $C_{23}H_{45}Cl_3NP_2Rh$: C, 45.52; H, 7.47; N, 2.31. Found: C, 45.26; H, 7.29; N, 2.37.

Preparation of *trans*-Rh^{III}Cl(CNXy)(η^2-O_2)$(PEt_3)_2$ (4b). A 10 mL Schlenk flask was charged with **1b** (50 mg, 0.099 mmol) dissolved in 4 mL of Et_2O. With vigorous stirring, the headspace was purged with O_2 for 1 min, and after removing the O_2 stream the solution was allowed to stir for an additional 5 min, leaving a dull yellow-brown solution. The solvent was removed in vacuo to give a brown solid, which was redissolved in Et_2O and transferred to a scintillation vial in the glovebox. Solvent was removed again in vacuo, and the resulting solid was washed with 2 mL of hexane and dried in vacuo briefly (<30 min). NMR spectra show ca. 7% of **1b**, though the microanalytical data and IR spectrum suggest high purity for the isolated solid. Yield: 45 mg (85%). ^{1}H NMR (500 MHz, C_6D_6) δ/ppm: 6.73−6.79 (m, 1H), 6.66−6.69 (m, 2H), 2.35 (s, 6H), 1.90 (m, 6H), 1.72 (m, 6H), 1.09 (quintet, 18H). $^{31}P\{^1H\}$ NMR (121.5 MHz, C_6D_6) δ/ppm: 26.3 (d, $^1J_{Rh-P}$ = 87 Hz). UV−vis (THF): λ/nm (ε/M^{-1} cm^{-1}) 243 (40 000). IR (Nujol): $\tilde{\nu}_{C\equiv N}$ = 2122 cm^{-1}, $\tilde{\nu}_{O-O}$ = 876 cm^{-1}. Anal. Calcd for $C_{21}H_{39}ClNO_2P_2Rh$: C, 46.90; H, 7.31; N, 2.60. Found: C, 46.81; H, 7.24; N, 2.55.

Preparation of *trans*-Rh^{III}(CNAd)Cl(η^2-O_2)$(PEt_3)_2$ (4c). A solution of **1c** (50 mg, 0.093 mmol) in 4 mL of Et_2O was prepared in a 10 mL Schlenk flask. The headspace was flushed with O_2 for 1 min with vigorous stirring, and after removing the O_2 flow stirring was continued for an additional 5 min. The resulting yellow-brown solution was concentrated in vacuo to give an olive green solid. In the glovebox, the solid was dissolved in Et_2O and transferred to a scintillation vial. Volatiles were removed in vacuo, and the product was washed with 2 mL of hexane before drying briefly in vacuo. Yield: 49 mg (92%). ^{1}H NMR (500 MHz, C_6D_6) δ/ppm: 1.93 (m, 6H), 1.82 (m, 6H), 1.76 (br, d, 6H), 1.64 (br, m, 3H), 1.15−1.28 (m, 24H). $^{31}P\{^1H\}$ NMR (121.5 MHz, C_6D_6) δ/ppm: 25.3 (d, $^1J_{Rh-P}$ = 89 Hz). UV−vis (THF): λ/nm (ε/M^{-1} cm^{-1}) 241 (23 000). IR (Nujol): $\tilde{\nu}_{C\equiv N}$ = 2135 cm^{-1}, $\tilde{\nu}_{O-O}$ = 877 cm^{-1}. Anal. Calcd for $C_{23}H_{45}ClNO_2P_2Rh$: C, 48.64; H, 7.99; N, 2.47. Found: C, 48.75; H, 7.75; N, 2.44.

O_2 Reduction Reactions of 2a−2c. All O_2 reduction reactions were executed and monitored in a screw-cap NMR tube with a PTFE septum seal. In all cases, the concentration of the hydride complex was 25 mM at the start of the reaction. Hydride complex **2a** (L = CO) was generated in situ by dissolving a sample of **1a** (7.0 mg, 0.017 mmol) in 0.35 mL of 1,4-dioxane and adding 0.35 mL of a 4.13 M solution of HCl in dioxane. For **2b** (L = CNXy) and **2c** (L = CNAd), an appropriate amount of the hydride was dissolved in 1,4-dioxane and the HCl/dioxane solution was added to produce a total volume of 0.7 mL with the desired concentration of HCl. Alternatively, the hydride complexes **2b** and **2c** could be generated in situ from **1b** and **1c** at no detriment to the observed reaction. After addition of the hydride complex and HCl, the headspace of the NMR tube was purged for ∼1 min with O_2 at atmospheric pressure. The contents of the tube were shaken vigorously to ensure complete mixing and periodically mixed throughout the course of the reactions, which were monitored by $^{31}P\{^1H\}$ NMR spectroscopy.

Addition of HCl to 4b to Generate 3b/5b. Complex **1b** (9.0 mg, 0.018 mmol, 1.0 equiv) was dissolved in 0.7 mL of THF-d_8 in a screw-cap, septum-sealed NMR tube. The headspace of the NMR tube was purged with O_2 (1 atm) and manually shaken to mix, generating a

dx.doi.org/10.1021/ic300279z | Inorg. Chem. 2012, 51, 7192−7201

Table 1. Crystallographic Summary for Complexes 2b, 3b, 4b, and 5c

	2b	3b	4b	5c•CH_2Cl_2
formula	$C_{21}H_{40}Cl_2NP_2Rh$	$C_{21}H_{39}Cl_3NP_2Rh$	$C_{21}H_{39}ClNO_2P_2Rh$	$C_{24}H_{47}Cl_5NOP_2Rh$
fw, g/mol	542.29	576.73	537.83	707.73
temp./K	100(2)	200(2)	100(2)	100(2)
color	colorless	yellow	brown	yellow
cryst syst	monoclinic	orthorhombic	monoclinic	monoclinic
space group	*Cc*	$Pna2_1$	$P2_1/n$	$P2_1/n$
a/Å	11.4479(12)	20.1861(8)	15.214(2)	14.7676(19)
b/Å	14.6692(15)	10.3567(4)	11.4156(18)	11.0440(14)
c/Å	15.4302(15)	12.9174(5)	15.778(3)	19.617(2)
β/deg	93.787(2)	90	113.796(2)	90.952(2)
V/Å^3	2585.6(5)	2700.53(18)	2507.3(7)	3199.0(7)
Z	4	4	4	4
no. of reflns	25 388	61 558	57 744	68 331
no. of unique reflns	6906	8130	7671	9363
R_{int}	0.0272	0.0353	0.0324	0.0722
R_1[a] (all data)	0.0229	0.0203	0.0246	0.0736
wR_2[b] (all data)	0.0465	0.0457	0.0508	0.1624
R_1 [$(I > 2\sigma)$]	0.0205	0.0183	0.0195	0.0609
wR_2 [$(I > 2\sigma)$]	0.0452	0.0442	0.0472	0.1564
GOF[c]	1.042	1.075	1.042	1.220
Flack-*x* param	−0.030(14)	0.638(13)		

[a] $R_1 = \Sigma||F_o| - |F_c||/\Sigma|F_o|$. [b] $wR_2 = (\Sigma(w(F_o^2 - F_c^2)^2)/\Sigma(w(F_o^2)^2))^{1/2}$. [c] GOF $= (\Sigma w(F_o^2 - F_c^2)^2/(n-p))^{1/2}$, where *n* is the number of data and *p* is the number of parameters refined.

dull yellow solution of **4b**. A solution of HCl in dioxane (4.2 M, 13 μL, 0.054 mmol, 3.0 equiv) was added via syringe, resulting in an immediate color change to bright yellow. A $^{31}P\{^1H\}$ NMR spectrum recorded immediately after addition of HCl showed a mixture of **5b** (80%), **3b** (17%), and ∼3% of unidentified side products. The solution was transferred to a scintillation vial and concentrated in vacuo, and the resulting residue was washed with hexane and dried in vacuo. Spectral data for **5b**: ^1H NMR (500 MHz, CD_3CN) *δ*/ppm: ∼7.3 (m, 1H, overlapped with **3b**), 7.22 (m, 2H, overlapped with **3b**), 5.92 (br, s, 2H), 2.58 (s, 6H), 2.17 (m, 12H), 1.18 (quintet, 18H). $^{31}P\{^1H\}$ NMR (121.5 MHz, CD_3CN) *δ*/ppm: 19.1 (d, $^1J_{Rh-P}$ = 74 Hz).

Addition of HCl to 4c to Generate 3c/5c. A solution of **1c** (9.0 mg, 0.017 mmol, 1.0 equiv) in 0.7 mL of THF-d_8 was prepared in a screw-cap NMR tube with septum seal. The headspace was purged with 1 atm of O_2 for 1 min, and upon shaking the contents changed to a dull olive color, which was shown to be complex **4c**. Addition of an HCl/dioxane solution (4.2 M, 12 μL, 0.050 mmol, 2.9 equiv) produced a bright yellow solution. Alternatively, the reaction can be executed starting with isolated **4c** with no additional O_2, and analysis of the headspace gases by gas chromatography shows no gaseous products after HCl addition. At this stage, $^{31}P\{^1H\}$ NMR indicates a mixture of **5b** (80%) and **3b** (20%). The solution was concentrated in vacuo, the product triturated with Et_2O/hexane, and the resulting yellow solid dried in vacuo. Spectral data for **5c**: ^1H NMR (500 MHz, C_6D_6) *δ*/ppm 6.58 (br, s, 2H), ∼2.22−2.41 (m, 12H, overlapped with **3c**), 2.21 (br, s, 6H), 1.74 (br, s, 3H), 1.14−1.39 (m, 24H, overlap with **3c**). $^{31}P\{^1H\}$ NMR (121.5 MHz, C_6D_6) *δ*/ppm: 17.4 (d, $^1J_{Rh-P}$ = 76 Hz).

X-ray Crystallographic Details. Single crystals of **2b** were obtained by cooling a saturated toluene/hexane solution to −20 °C, **3b** and **5c** crystallized from saturated CH_2Cl_2/hexane solutions at −20 °C, and crystals of **4b** formed by allowing O_2 to slowly diffuse into a hexane solution of **1b** at room temperature. Crystals of **3b**, **4b**, and **5c** were mounted on a Bruker three-circle goniometer platform equipped with an APEX detector, whereas crystals of **2b** were mounted on a Bruker four-circle goniometer platform with an APEX 2 detector. A graphite monochromator was employed for wavelength selection of the Mo K*α* radiation (*λ* = 0.71073 Å). Data were processed and refined using the program SAINT supplied by Siemens Industrial Automation. Structures were solved by Patterson methods or direct methods in SHELXS and refined by standard difference Fourier techniques in the SHELXTL program suite (6.10 v., Sheldrick G. M., Siemens Industrial Automation, 2000). Hydrogen atoms bonded to carbon were placed in calculated positions using the standard riding model and refined isotropically; all non-hydrogen atoms were refined anisotropically. In the structure of **2b**, the rhodium-bound hydrogen atom was tentatively located in the difference map and refined isotropically. The O−H hydrogen atoms in the structure of **5c** were also located in the difference map; they were restrained to a distance of 0.84 Å from the oxygen atom and refined isotropically. The structure of **3b** was refined as a racemic twin. In the structure of **5c**, the adamantyl group, one of the ethyl groups, and a solvent dichloromethane molecule were all modeled as two-part positional disorders. The corresponding 1−2 and 1−3 distances of all disordered parts were restrained to be identical, and rigid bond restraints were used on all disordered atoms. Crystallographic details for the structures of **2b**, **3b**, **4b**, and **5c** are summarized in Table 1.

RESULTS

Hydride Complexes. Hydride complexes *cis-trans*-$Rh^{III}Cl_2H(L)(PEt_3)_2$ (**2a−c**) were prepared by HCl addition to Rh^I complexes **1a−c**, as depicted in Scheme 1. Treatment of **1a** with a large excess of HCl results in growth of new NMR

Scheme 1

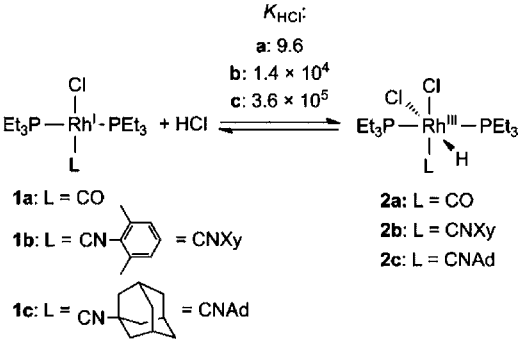

dx.doi.org/10.1021/ic300279z | Inorg. Chem. 2012, 51, 7192−7201

features attributable to **2a**. HCl addition to **1a** to form **2a** is reversible,[59] such that removal of HCl from **2a** results in complete reversion to **1a**. Complexes **2b** and **2c** featuring isocyanide ligands have not been previously described, though an isolated example of a close relative prepared by hydride transfer from an alcoholic reaction medium is known.[60] Hydride complexes **2b** and **2c** were found to form quantitatively upon treatment of **1b** and **1c** with HCl. Furthermore, these complexes are isolable and can be obtained in pure form as colorless solids. Characteristic NMR features, similar to those described for **2a**, are observed for **2b** and **2c** as well and are summarized in the Experimental Section.

The stereochemistry of **2b** was confirmed by single-crystal X-ray diffraction. The structure of the complex is shown in Figure 1. The geometry of the Rh^{III} center is octahedral with a trans

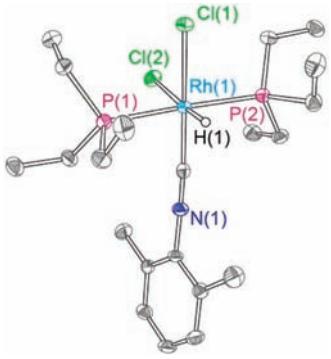

Figure 1. Thermal ellipsoid plot of **2b**, shown at the 50% probability level. All carbon-bound hydrogen atoms are omitted for clarity. Data were collected at 100(2) K.

arrangement of the two PEt_3 ligands and a cis arrangement of the two Cl^- ligands. Of note is the disparity of the two Rh−Cl bond distances. The strong trans influence of the hydride ligand causes the Rh(1)−Cl(2) distance [2.4947(5) Å] to be substantially longer than the Rh(1)−Cl(1) distance [2.4041(5) Å]. The stereochemistry of **2b** is consistent with the known stereochemical preference for HCl addition to square-planar M^I centers,[61] and this precedent, coupled with the similarities in the NMR features, led us to conclude that **2a** and **2c**, which were not crystallographically characterized, are isostructural with **2b.**

Addition of HCl to **1a**−**c** establishes the equilibrium shown in Scheme 1. The equilibrium constant for the reaction (K_{HCl} = [**2**]/[**1**][HCl]) was determined directly by addition of a known concentration of HCl to a 1,4-dioxane solution of **1a**. Integration of the $^{31}P\{^1H\}$ NMR spectrum furnished the equilibrium concentrations of **1a** and **2a**. The equilibrium constants for the **1b**/**c** to **2b**/**c** conversions were too large to be easily determined by direct addition of HCl to solutions of the starting complexes. Thus, a thermodynamic cycle connecting HCl and the weaker acid, 2,6-lutinidium hydrochloride, was constructed. These studies were conducted in acetonitrile, owing to the considerable solubility of protonated amine bases and ready availability of the relevant thermodynamic data in that solvent. Complex **1a** is completely unreactive to 2,6-lutidinium hydrochloride, so it was not possible to confirm its K_{HCl} value by this method. By using 2,6-lutinidium hydrochloride as the acid source in acetonitrile, an equilibrium between the Rh^I complex (**1b**/**c**) and Rh^{III} hydride (**2b**/**c**) was established. By coupling this measured equilibrium constant with the known pK_as of 2,6-lutidinium (14.13)[62] and HCl (8.9)[63] in acetonitrile,[51,64] the K_{HCl} values were determined and are tabulated in Scheme 1. Though the measured value of K_{HCl} will somewhat be dependent on solvent choice, the disparate solvent media for addition reactions of **1a** and **1b**/**c** cannot account for the dramatic changes in K_{HCl} that occur upon ligand substitution.

ORR Activity. Hydride complexes **2a**−**c** react with O_2, in the presence of additional HCl, as summarized in Scheme 2;

Scheme 2

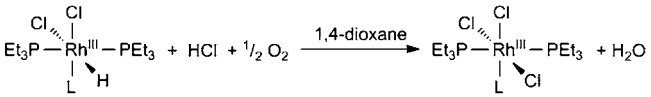

2a: L = CO
2b: L = CNXy
2c: L = CNAd

3a: L = CO
3b: L = CNXy
3c: L = CNAd

though the O_2 stoichiometry is ill defined (vide infra), the only two products readily identified by spectroscopic methods, **3a**−**c** and water, are quantifiable. In all cases, the final outcome of the reaction between the hydride complex and O_2 and HCl is the respective *trans*-$Rh^{III}Cl_3(L)(PEt_3)_2$, **3a**−**c**, which is produced cleanly. Products **3a**−**c** were prepared independently by $PhICl_2$ oxidation of Rh^I complexes **1a**−**c**, allowing the identities of the final products formed in the reactions of Scheme 2 to be ascertained unequivocally. Complexes **3a**−**c** possess similar $^{31}P\{^1H\}$ spectral features, and together with the X-ray crystal structure results of Figure 2, a trans arrangement of the PEt_3 ligands and the corresponding meridional arrangement of Cl^- ligands in these products are established.

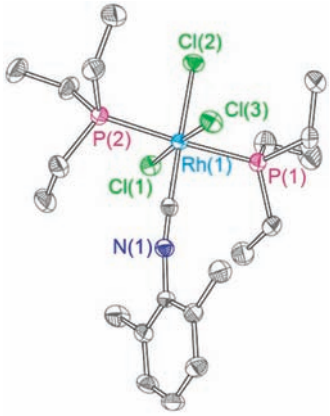

Figure 2. Thermal ellipsoid plot of **3b**, shown at the 50% probability level. All hydrogen atoms are omitted for clarity. Data were collected at 200(2) K.

The reaction progression of hydride **2a** significantly deviates from that of **2b** and **2c**. Figure 3 shows the evolution of the $^{31}P\{^1H\}$ NMR spectra upon treatment of **2a** with HCl (2.1 M) and O_2 (ca. 0.2 atm) in 1,4-dioxane at room temperature. Over a long time course, the resonance attributed to **2a** (27.0 ppm, $^1J_{Rh-P}$ = 80 Hz) gives rise exclusively to the resonance for **3a** (19.9 ppm, $^1J_{Rh-P}$ = 72 Hz). In parallel to the dirhodium system,[49,51] no intermediates are spectroscopically observed along the ORR conversion.

dx.doi.org/10.1021/ic300279z | *Inorg. Chem.* 2012, 51, 7192−7201

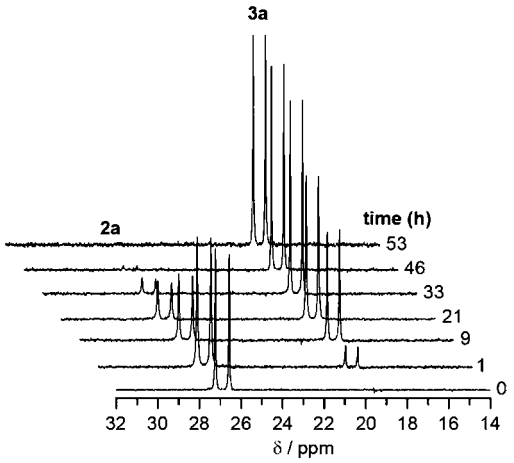

Figure 3. Temporal evolution of the $^{31}P\{^{1}H\}$ NMR spectra when **2a**, in the presence of 2.1 M HCl, is treated with ca. 0.2 atm of O_2 at room temperature. Spectra were collected at the time intervals depicted on the right of the plot. Resonances attributed to **2a** and **3a** are labeled.

As shown in Figure 4, conversion of **2c** in the presence of HCl (77 mM) and O_2 (1 atm) in 1,4-dioxane to **3c** is also slow.

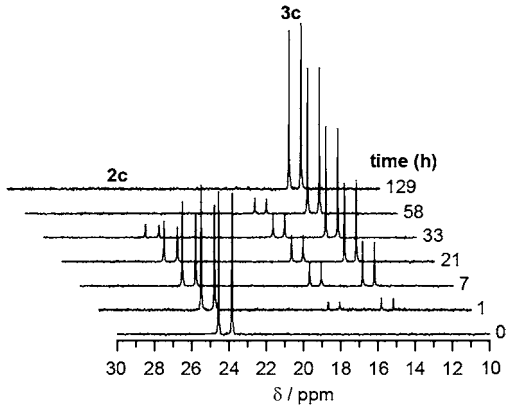

Figure 4. Time-resolved $^{31}P\{^{1}H\}$ NMR spectra when **2c**, in the presence of 77 mM HCl, is treated with 1 atm of O_2 at room temperature. Spectra were collected at the time intervals depicted on the right of the plot. Resonances attributed to **2c** and **3c** are labeled.

However, growth of an intermediate species in the $^{31}P\{^{1}H\}$ NMR spectrum is clearly observed. Whereas a $^{31}P\{^{1}H\}$ NMR doublet of **2c** (24.2 ppm, $^{1}J_{Rh-P}$ = 87 Hz) is observed at early times and of **3c** (14.5 ppm, $^{1}J_{Rh-P}$ = 78 Hz) is observed at late times, a unique species, with a chemical shift of 17.4 ppm and $^{1}J_{Rh-P}$ = 75 Hz, is apparent at intermediate times. Under identical conditions a very similar outcome is observed for **2b**; as shown in Figure S1, Supporting Information, an intermediate species appears during conversion of **2b** to **3b.** Figures S2 and S3, Supporting Information, demonstrate qualitatively the effect of augmenting the acid concentration to 250 mM on the overall reaction progress for **2b** and **2c**, respectively. The observations are generally similar, though in the case of **2b** increasing [HCl] results in a much smaller amount of the intermediate species along the path to forming **3b**; after the first 2 h of conversion only **2b** and **3b** are present. In addition, the time required to completely consume hydride **2b** is substantially longer at higher acid concentrations. For **2c**, increasing the concentration of HCl also lengthens the reaction time but the intermediate is observed in comparable amounts. As detailed below, an alternate reaction strategy furnishes this intermediate in much higher yields, ultimately allowing us to identify it as a Rh^{III} aqua complex.

Peroxy Intermediates. Addition of 1 atm of O_2 to a solution of **1a** produces only a small amount of a new product, **4a**, with mostly **1a** remaining. Product **4a**, which forms in <5% yield under these conditions, shows a slightly downfield-shifted $^{31}P\{^{1}H\}$ resonance (30.0 ppm) with a smaller $^{1}J_{Rh-P}$ coupling constant (82 Hz) relative to that of **1a**. Over a period of 1 week, the compound decomposes and O═PEt_3 and an intractable mixture of metal-containing products is observed. In contrast, treatment of **1b**/**c** with O_2 at 1 atm leads to clean, quantitative formation of *trans*-$Rh^{III}Cl(L)(\eta^2\text{-}O_2)(PEt_3)_2$ (**4b**, L = CNXy; **4c**, L = CNAd) as illustrated in Scheme 3. Though these

Scheme 3

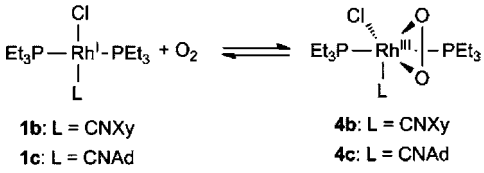

complexes suffer from limited solution stability, again decomposing to O═PEt_3 and a mixture of rhodium-containing products, the peroxo complexes can be isolated in pure form in the solid state and do persist long enough in solution to characterize their spectral properties and reactivity. Isolated solids of **4b**/**4c** give rise to nearly identical O−O bond-stretching frequencies in their infrared spectra ($\tilde{\nu}_{O-O}$ = 876 cm^{-1} for **4b** and 877 cm^{-1} for **4c**); these values are suggestive of an O−O single bond.[65] Figures S14 and S15, Supporting Information, collect overlaid partial IR spectra for **1b**/**c**−**4b**/**c**, which show that the region of 800−1000 cm^{-1} is essentially transparent for all other complexes, allowing the O−O stretching frequency for **4b**/**c** to be easily identified. The assignments of these stretching frequencies are further validated by their similarity to some well-characterized palladium[66,67] and rhodium[68,69] peroxo complexes and their good correlation with the observed O−O bond length,[70] which is given below.

The X-ray crystal structure of **4b**, shown in Figure 5, confirms that O_2 binds in a η^2-peroxo motif. The geometry about the Rh^{III} center approximates trigonal bipyramidal if the midpoint of the O−O vector is taken to occupy a coordination site. As established from the $^{31}P\{^{1}H\}$ NMR spectrum the two

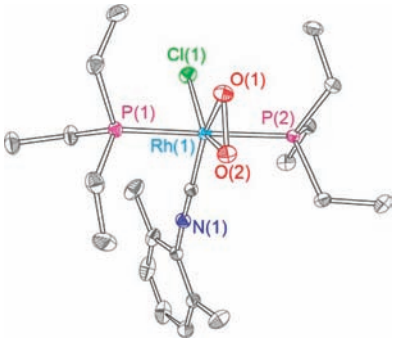

Figure 5. Thermal ellipsoid plot of **4b**, shown at the 50% probability level. All hydrogen atoms are omitted for clarity. Data were collected at 100(2) K.

dx.doi.org/10.1021/ic300279z | *Inorg. Chem.* 2012, 51, 7192−7201

PEt_3 ligands remain trans to one another, occupying the apical positions of the trigonal bipyramid. The O(1)−O(2) internuclear distance of 1.4413(12) Å is consistent with the formulation of an O_2^{2-} ligand with an O−O single bond.[40,51,70] Although **4c** was not structurally characterized, its nearly identical spectral features to those of **4b** point to an analogous structure for **4c**.

With synthetic routes to **4b** and **4c** in hand, we interrogated the reactivity of the compounds with HCl; identical outcomes are obtained whether or not additional O_2 is present. This reactivity is summarized in Scheme 4. Whereas treatment of **4b** and **4c** with a single equivalent of HCl produces an intractable mixture of Rh^{III} products, use of excess HCl cleanly generates a mixture of two products. After 20 min, the major product (ca. 80%) is the same intermediate observed above in the O_2 reduction experiments with the balance accounted for by **3b/c**. $^{31}P\{^1H\}$ and ^1H NMR spectra indicate that these are the only two diamagnetic products containing phosphorus and/or hydrogen nuclei. Moreover, the IR spectra of solid product (vide infra), isolated without any purification, shows only features attributed to these two diamagnetic products, discounting the presence of substantial paramagnetic impurities. The intermediate gradually converts to **3b/c** over time, in line with the observations in the previous section for the O_2 reduction experiments, where **3b/c** are formed as the exclusive products when the aqua intermediate disappears. Gas chromatographic analysis of the headspace gas, immediately following HCl addition to anaerobic solutions of **4b/c**, shows no evidence for gaseous products formed during this reaction, indicating that O_2 is not a reaction product. As such, the fate of the second oxygen atom in the peroxo remains unclear, but mechanisms which could result in production of 1/2 O_2 can be ruled out.

Scheme 4

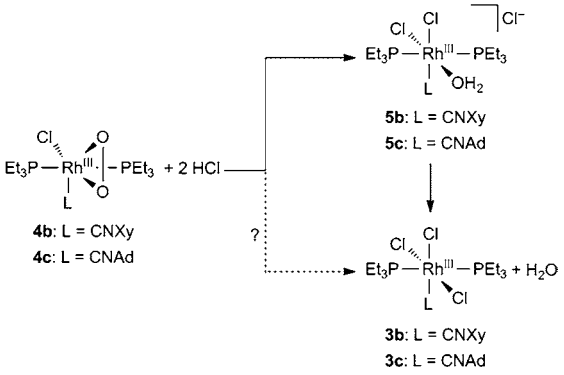

Having established a route to prepare the intermediate in appreciable quantities, interrogation of the compound with a variety of experimental methods leads to its unequivocal identification as the aqua complex, *cis-trans*-$[Rh^{III}(OH_2)Cl_2(L)(PEt_3)_2]Cl$ (**5b**, L = CNXy; **5c**, L = CNAd). The IR spectrum of an isolated solid mixture of **5b/c** and **3b/c** shows only stretches attributed to the PEt_3 and isocyanide ligands. The region between 800 and 1000 cm^{-1} is notably barren, suggesting the absence of an O−O bond in **5b/c** and discounting the formulation of these intermediates as hydroperoxo complexes. Furthermore, in the absence of HCl the ^1H NMR spectra of **5b/c**, in addition to the expected resonances arising from PEt_3 and the respective isocyanide, show an additional singlet that integrates to two protons at 5.92 (**5b**, CD_3CN) and 6.58 ppm (**5c**, C_6D_6). With HCl present, these resonances are broadened considerably and coalesce with the resonance for free HCl. The positions of these new resonances, their slightly broadened line shapes, and their rapid exchange with HCl on the NMR time scale suggest O−*H* protons. We also verified that **5c** cleanly converts to **3c** in C_6D_6 in the absence of HCl or O_2. Over a period of ca. 24 h, the NMR features of **5c** disappear, with concomitant growth of the peaks for **3c** as well as a broad singlet at 0.60 ppm, which we attribute to free H_2O. The broadening of this water peak and the slight shift from the 0.40 ppm chemical shift of H_2O in C_6D_6[71] indicate a weak interaction of the liberated water with **3c**.

All spectroscopic results were confirmed with the solution of the single-crystal X-ray structure of **5c**. Figure 6 shows two views of the structure of **5c**. In Figure 6a, the cation *cis-trans*-$[Rh^{III}(CNAd)(OH_2)Cl_2(PEt_3)_2]^+$ is depicted, which confirms the stereochemistry about the Rh^{III} center, where a trans arrangement of the two PEt_3 ligands and a cis arrangement of the two Cl− ligands persists. In Figure 6b, the structure is extended to show the outer-sphere Cl^- counterion as well as a neighboring molecule of **5c** that is related by a crystallographic inversion center. This view clearly shows a series of hydrogen-bonding interactions between the aqua protons and the outer-sphere Cl^- anions that stabilize the structure and give rise to a dimeric motif in the solid state. The hydrogen-bonding donor−

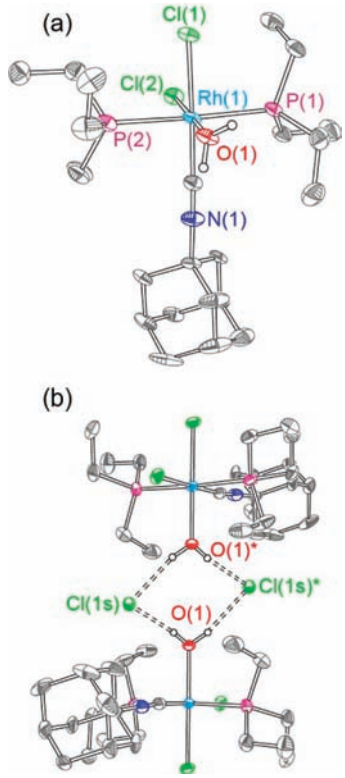

Figure 6. Thermal ellipsoid plots of **5c**, shown at the 50% probability level. All carbon-bound hydrogen atoms and solvent molecules are omitted for clarity. Data were collected at 100(2) K. (a) Cation is shown with the outer-sphere Cl^- omitted. (b) Counterion is included as well as a second molecule of **5c** generated by a crystallographic inversion center. Dashed lines indicate located hydrogen bonds, and atoms labeled with an asterisk (*) are symmetry equivalents of those with conventional labels.

dx.doi.org/10.1021/ic300279z | *Inorg. Chem.* 2012, 51, 7192−7201

acceptor distance between O(1) and Cl(1s) is 2.948(3) Å, whereas the distance is 3.056(3) Å between O(1) and the symmetry-generated equivalent of Cl(1s). This reveals a slight asymmetry in the two crystallographically independent hydrogen-bonding interactions.

In summary, treatment of **4b/c** with HCl results in rapid cleavage of the O−O bond and instantaneous generation of aqua intermediate **5b/c**, which liberates H_2O and forms **3b/c** irrespective of the presence of O_2 and HCl. It is not definitive at this stage whether conversion of peroxo complex **4b/c** to $Rh^{III}Cl_3$ complex **3b/c** necessarily proceeds through the aqua intermediate **5b/c** or if direct conversion is possible (dashed arrow in Scheme 4). It seems likely that such a direct pathway occurs, since there is a ca. 20% population of **3b/c** immediately after HCl addition, and conversion of **5b/c** to **3b/c** requires ∼24 h, suggesting there is a route to **3b/c** that does not require intermediacy of aqua complexes **5b/c**. Ultimately, detailed reaction kinetics will be turned to to distinguish these possibilities.

DISCUSSION

Alteration of a single neutral donor ligand can have a profound effect on O_2 activation and reduction by late metal molecular complexes. The dramatic effect of the ligand environment is manifested most profoundly in the equilibrium constant for HCl addition, K_{HCl}, an important parameter for O_2 activation, particularly when a HXRE mechanism is operative.[44−46,51] The strongly π-acidic CO-supporting ligand of **1a** renders the Rh^I center comparatively electron poor, and a K_{HCl} of 9.6 is observed. The small value of K_{HCl} precludes isolation of hydride complex **2a**, and in the absence of HCl, reversion to **1a** occurs with facility. Upon changing L to substituted isocyanides, HCl addition is strongly favored (see Scheme 1) and isolation of hydrides **2b/c** is readily achieved. Similar trends are observed for addition of O_2 to **1a−c** to generate peroxo complexes **4a−c**. For **1a**, addition of 1 atm of O_2 generates only a small amount of the presumed peroxo complex **4a**, whereas quantitative formation of **4b/c** is observed under identical conditions. The thermodynamic metrics for HCl addition, coupled with the qualitative observations on O_2 addition, readily demonstrate that the electronic environment of the rhodium center can be significantly altered by simple ligand substitution.

The O_2-reduction chemistry of *cis-trans*-$Rh^{III}Cl_2H(L)(PEt_3)_2$ (**2a−c**) is quite general. In all cases, treatment of the hydride with excess HCl and O_2 leads to smooth conversion to *trans*-$Rh^{III}Cl_3(L)(PEt_3)_2$ (**3a−c**) with concomitant formation of H_2O, monometallic analogues to previously reported bimetallic systems.[49] Though an intermediate is not observed for **2a** by traditional spectroscopic techniques, the aqua complex $[Rh^{III}(OH_2)Cl_2(L)(PEt_3)_2]Cl$ (**5b/c**) appears during the course of the reaction of **2b/c** to **3b/c**. Identification of **5b/c** demonstrates that O_2 is being reduced to water in these systems, though it is unclear at this stage if there is a mechanistic significance of the bound aqua complex, which has not been detected for the ORR of bimetallic systems. Also worth noting is that the absence of the intermediate's appearance in the aerobic conversion of **2a** to **3a** may not have mechanistic significance, given the drastically different conditions (much higher HCl concentration) required to study complex **2a**.

The reaction times for O_2 reduction by the monometallic systems described here are substantially longer than those required for bimetallic complexes. For hydride **2a** (L = CO), high concentrations of HCl are required to ensure **2a** as the majority species, so meaningful comparisons of qualitative reaction rates cannot be easily made for this complex. However, hydrides **2b/c** do react under identical conditions to those investigated for the dirhodium hydrides, and reaction times of ∼4−5 days are required, as compared to a few hours for dirhodium complexes. These observations suggest a possible benefit of bimetallic cooperativity for ORR promoted by late transition metal systems, but the comparison is muddled by ligand electronic effects, so additional studies of detailed reaction kinetics will be required to fully understand bimetallic effects in this chemistry.

As η^2-peroxo species are keystones to ORR, especially for reactions proceeding by a HXRE mechanism, peroxo complexes **4b/c** were independently prepared by pressurizing **1b/c** with 1 atm of O_2, and their reactivity was investigated with HCl under both aerobic and anaerobic conditions. Analogous reactions have been interrogated on a series of closely related rhodium peroxo complexes,[68] though in these previous examples the hydroperoxo was stable enough to be observed and crystallized below room temperature, and further reaction with HCl liberated hydrogen peroxide and not water. These studies are especially valuable inasmuch as the dirhodium peroxo species are not synthetically accessible,[51] and thus, examination of peroxo reactivity in the context of this original system has not been feasible. The peroxo complexes described here react rapidly with excess HCl, forming a mixture of aqua complexes **5b/c** and $Rh^{III}Cl_3$ complexes **3b/c** before final conversion to **3b/c**. Even at early time points, **3b/c** and **5b/c** are the only two species observed spectroscopically, indicating facile cleavage of the O−O bond under these conditions. It is reasonable to assume that a hydroperoxo intermediate forms initially upon reaction with HCl, given the reactivity of other late metal peroxo systems.[51,68,72,73] However, in the case of the rhodium complexes described here, such hydroperoxo complexes are apparently too unstable to observe, as even a single equivalent of HCl added to **4b/c** fails to produce any spectroscopic features that can be confidently assigned to a hydroperoxo complex. Several key details of this O−O bond-cleaving transformation remain unclear, but some possibilities can be ruled out. Notably, O_2 gas is not produced upon HCl-induced oxygen−oxygen bond scission of **4b/c**. This observation rules out a pathway in which H_2O_2, liberated by protonolysis, disproportionates into H_2O and 1/2 O_2 and also eliminates any other possibility, such as a bimolecular pathway, which would result in liberating 1/2 O_2. One possibility that cannot be ruled out is that protonation of a putative hydroperoxo releases water and leaves an unstable high-valent oxo species which rapidly decomposes, presumably by reaction with solvent. The nature of this decomposition is not apparent from any of the available data, though rhodium-containing products other than **3b/c** and **5b/c** are not observed given the quantitative yields for the overall reactions. Such reactivity with acids has been characterized for some other synthetic metal−hydroperoxo complexes, where a high-valent oxo complex is likewise observed or inferred upon acid-induced O−O bond heterolysis.[74−76] Notwithstanding, the reactivity of peroxo complexes **4b/c** with HCl, which generates water and trichloro complexes **3b/c** as the final outcome, bespeaks to the plausibility of an HXRE mechanism for ORR by hydride complexes **2b/c**. Forthcoming kinetic studies on these and related complexes will reveal whether HXRE is the preferred mechanism for the reactivity of hydrides **2b/c** or if other

dx.doi.org/10.1021/ic300279z | Inorg. Chem. 2012, 51, 7192−7201

mechanism(s) prevail. These results set the stage for a thorough and systematic mechanistic interrogation of O_2 activation and reduction by monometallic rhodium hydride complexes.

To conclude, monometallic Rh^{III} hydride complexes, in the presence of HCl, quantitatively reduce one-half of an equivalent of O_2 to water. The chemistry of independently prepared peroxo congeners points to HXRE as the mechanism of ORR. Mechanistic studies underway to define the precise mechanism of ORR are bolstered by the ease with which O_2 reactivity can be tuned by ligand design of the monometallic rhodium platform.

■ ASSOCIATED CONTENT

Ⓢ Supporting Information

$^{31}P\{^1H\}$ NMR spectra for aerobic conversion of **2b/c** and HCl to **3b/c**, electronic spectra for complexes **1a−c**, **2b/c**, **3a−c**, and **4b/c**, partial IR spectra for **1b/c−4b/c**, and crystallographic information file (CIF). This material is available free of charge via the Internet at http://pubs.acs.org.

■ AUTHOR INFORMATION

Corresponding Author

*E-mail: nocera@mit.edu.

Notes

The authors declare no competing financial interest.

■ ACKNOWLEDGMENTS

This work was supported by NSF grant CHE-1112154. Grants from the NSF also supported the MIT Department of Chemistry Instrumentation Facility (CHE-9808061 and DBI-9729592). T.S.T. acknowledges the Fannie and John Hertz Foundation for a graduate research fellowship.

■ REFERENCES

(1) Barber, J. *Chem. Soc. Rev.* **2009**, *38*, 185−196.
(2) Barber, J. *Philos. Trans. R. Soc. A* **2007**, *365*, 1007−1023.
(3) Cook, T. R.; Dogutan, D. K.; Reece, S. Y.; Surendranath, Y.; Teets, T. S.; Nocera, D. G. *Chem. Rev.* **2010**, *110*, 6474−6502.
(4) Lewis, N. S.; Nocera, D. G. *Proc. Natl. Acad. Sci. U.S.A.* **2006**, *103*, 15729−15735.
(5) Kaila, V. R. I.; Verkhovsky, M. I.; Wikström, M. *Chem. Rev.* **2010**, *110*, 7062−7081.
(6) Baik, M.-H.; Newcomb, M.; Friesner, R. A.; Lippard, S. J. *Chem. Rev.* **2003**, *103*, 2385−2419.
(7) Himes, R. A.; Barnese, K.; Karlin, K. D. *Angew. Chem., Int. Ed.* **2010**, *49*, 6714−6716.
(8) Collman, J. P.; Boulatov, R.; Sunderland, C. J.; Fu, L. *Chem. Rev.* **2004**, *104*, 561−588.
(9) Rosenthal, J.; Nocera, D. G. *Acc. Chem. Res.* **2007**, *40*, 543−553.
(10) Rosenthal, J.; Nocera, D. G. *Prog. Inorg. Chem.* **2007**, *55*, 483−544.
(11) McGuire, R., Jr.; Dogutan, D. K.; Teets, T. S.; Suntivich, J.; Shao-Horn, Y.; Nocera, D. G. *Chem. Sci.* **2010**, *1*, 411−414.
(12) Dogutan, D. K.; Stoian, S. A.; McGuire, R., Jr.; Schwalbe, M.; Teets, T. S.; Nocera, D. G. *J. Am. Chem. Soc.* **2011**, *133*, 131−140.
(13) Chang, C. J.; Deng, Y.; Shi, C.; Chang, C. K.; Anson, F. C.; Nocera, D. G. *Chem. Commun.* **2000**, 1355−1356.
(14) Chang, C. J.; Loh, Z.-H.; Shi, C.; Anson, F. C.; Nocera, D. G. *J. Am. Chem. Soc.* **2004**, *126*, 10013−10020.
(15) Collman, J. P.; Wagenknecht, P. S.; Hutchison, J. E. *Angew. Chem., Int. Ed.* **1994**, *33*, 1537−1554.
(16) Collman, J. P.; Fu, L.; Hermann, P. C.; Zhang, X. *Science* **1997**, *275*, 949−951.
(17) Halime, Z.; Kotani, H.; Li, Y.; Fukuzumi, S.; Karlin, K. D. *Proc. Natl. Acad. Sci. U.S.A.* **2011**, *108*, 13990−13994.
(18) Stahl, S. S. *Angew. Chem., Int. Ed.* **2004**, *43*, 3400−3420.
(19) Punniyamurthy, T.; Velusamy, S.; Iqbal, J. *Chem. Rev.* **2005**, *105*, 2329−2363.
(20) Kunisu, T.; Oguma, T.; Katsuki, T. *J. Am. Chem. Soc.* **2011**, *133*, 12937−12939.
(21) Frazier, C. P.; Engelking, J. R.; de Alaniz, J. R. *J. Am. Chem. Soc.* **2011**, *133*, 10430−10433.
(22) Liu, L.; Yu, M.; Wayland, B. B.; Fu, X. *Chem. Commun.* **2010**, *46*, 6353−6355.
(23) Li, H.; Wei, W.; Xu, Y.; Zhang, C.; Wan, X. *Chem. Commun.* **2011**, *47*, 1497−1499.
(24) Fries, P.; Halter, D.; Kleinschek, A.; Hartung, J. *J. Am. Chem. Soc.* **2011**, *133*, 3906−3912.
(25) Jiang, B.; Feng, Y.; Ison, E. A. *J. Am. Chem. Soc.* **2008**, *130*, 14462−14464.
(26) Izawa, Y.; Pun, D.; Stahl, S. S. *Science* **2011**, *333*, 209−213.
(27) Chuang, G. J.; Wang, W.; Lee, E.; Ritter, T. *J. Am. Chem. Soc.* **2011**, *133*, 1760−1762.
(28) Zhang, J.; Khaskin, E.; Anderson, N. P.; Zavalij, P. Y.; Vedernikov, A. N. *Chem. Commun.* **2008**, 3625−3627.
(29) Roberts, H. L.; Symes, W. R. *J. Chem. Soc. A* **1968**, 1450−1453.
(30) Johnston, L. E.; Page, J. A. *Can. J. Chem.* **1969**, *47*, 4241−4246.
(31) Gillard, R. D.; Heaton, B. T.; Vaughan, D. H. *J. Chem. Soc. A* **1970**, 3126−3130.
(32) Endicott, J. F.; Wong, C.-L.; Inoue, T.; Natarajan, P. *Inorg. Chem.* **1979**, *18*, 450−454.
(33) Atlay, M. T.; Preece, M.; Strukul, G.; James, B. R. *J. Chem. Soc., Chem. Commun.* **1982**, 406−407.
(34) Atlay, M. T.; Preece, M.; Strukul, G.; James, B. R. *Can. J. Chem.* **1983**, *61*, 1332−1338.
(35) Bakac, A. *J. Am. Chem. Soc.* **1997**, *119*, 10726−10731.
(36) Thyagarajan, S.; Incarvito, C. D.; Rheingold, A. L.; Theopold, K. H. *Chem. Commun.* **2001**, 2198−2199.
(37) Cui, W.; Wayland, B. B. *J. Am. Chem. Soc.* **2006**, *128*, 10350−10351.
(38) Wick, D. D.; Goldberg, K. I. *J. Am. Chem. Soc.* **1999**, *121*, 11900−11901.
(39) Konnick, M. M.; Gandhi, B. A.; Guzei, I. A.; Stahl, S. S. *Angew. Chem., Int. Ed.* **2006**, *45*, 2904−2907.
(40) Denney, M. C.; Smythe, N. A.; Cetto, K. L.; Kemp, R. A.; Goldberg, K. I. *J. Am. Chem. Soc.* **2006**, *128*, 2508−2509.
(41) Szajna-Fuller, E.; Bakac, A. *Inorg. Chem.* **2010**, *49*, 781−785.
(42) Keith, J. M.; Nielson, R. J.; Oxgaard, J.; Goddard, W. A., III *J. Am. Chem. Soc.* **2005**, *127*, 13172−13179.
(43) Keith, J. M.; Muller, R. P.; Kemp, R. A.; Goldberg, K. I.; Goddard, W. A., III; Oxgaard, J. *Inorg. Chem.* **2006**, *45*, 9631−9633.
(44) Popp, B. V.; Stahl, S. S. *J. Am. Chem. Soc.* **2007**, *129*, 4410−4422.
(45) Konnick, M. M.; Stahl, S. S. *J. Am. Chem. Soc.* **2008**, *130*, 5753−5762.
(46) Konnick, M. M.; Decharin, N.; Popp, B. V.; Stahl, S. S. *Chem. Sci* **2011**, *2*, 326−330.
(47) Decharin, N.; Stahl, S. S. *J. Am. Chem. Soc.* **2011**, *133*, 5732−5735.
(48) Decharin, N.; Popp, B. V.; Stahl, S. S. *J. Am. Chem. Soc.* **2011**, *133*, 13268−13271.
(49) Teets, T. S.; Cook, T. R.; McCarthy, B. D.; Nocera, D. G. *J. Am. Chem. Soc.* **2011**, *133*, 8114−8117.
(50) Teets, T. S.; Cook, T. R.; McCarthy, B. D.; Nocera, D. G. *Inorg. Chem.* **2011**, *50*, 5223−5233.
(51) Teets, T. S.; Nocera, D. G. *J. Am. Chem. Soc.* **2011**, *133*, 17796−17806.
(52) Keith, J. M; Teets, T. S.; Nocera, D. G. Submitted for publication.
(53) Look, J. L.; Wick, D. D.; Mayer, J. M.; Goldberg, K. I. *Inorg. Chem.* **2009**, *48*, 1356−1369.

(54) Gray, T. G.; Veige, A. S.; Nocera, D. G. *J. Am. Chem. Soc.* **2004**, *126*, 9760−9768.
(55) Chatt, J.; Shaw, B. L. *J. Chem. Soc. A* **1966**, 1437−1442.
(56) Sasaki, T.; Nakanishi, A.; Ohno, M. *J. Org. Chem.* **1981**, *46*, 5445−5447.
(57) Al-Jibori, S.; Crocker, C.; Shaw, B. L. *J. Chem. Soc., Dalton Trans.* **1981**, 319−321.
(58) Intille, G. M. *Inorg. Chem.* **1972**, *11*, 695−702.
(59) Conkie, A.; Ebsworth, E. A. V.; Mayo, R. A.; Moreton, S. *J. Chem. Soc., Dalton Trans.* **1992**, 2951−2954.
(60) Masters, C.; Shaw, B. L. *J. Chem. Soc. A* **1971**, 3679−3686.
(61) Vaska, L. *J. Am. Chem. Soc.* **1966**, *88*, 5325−5327.
(62) Kaljurand, I.; Kütt, A.; Sooväli, L.; Rodima, T.; Mäemets, V.; Leito, I.; Koppel, I. A. *J. Org. Chem.* **2005**, *70*, 1019−1028.
(63) Izutsu, K. *Electrochemistry in Nonaqueous Solutions*; Wiley-VCH: Weinheim, 2009; Chapter 3.
(64) Wilson, A. D.; Miller, A. J. M.; DuBois, D. L.; Labinger, J. A.; Bercaw, J. E. *Inorg. Chem.* **2010**, *49*, 3918−3926.
(65) Socrates, G. Peroxides and Hydroperoxides: −O−O−Group. *Infrared and Raman Characteristic Group Frequencies: Tables and Charts*, 3rd ed.; Wiley and Sons: Chichester, U.K., 2001; pp 105−106.
(66) Stahl, S. S.; Thorman, J. L.; Nelson, R. C.; Kozee, M. A. *J. Am. Chem. Soc.* **2001**, *123*, 7188−7189.
(67) Konnick, M. M.; Guzei, I. A.; Stahl, S. S. *J. Am. Chem. Soc.* **2004**, *126*, 10212−10213.
(68) Ahijado, M.; Braun, T.; Noveski, D.; Kocher, N.; Neumann, B.; Stalke, D.; Stammler, H.-G. *Angew. Chem., Int. Ed.* **2005**, *44*, 6947−6951.
(69) Carlton, L.; Mokoena, L. V.; Fernandes, M. A. *Inorg. Chem.* **2008**, *47*, 8696−8703.
(70) Cramer, C. J.; Tolman, W. B.; Theopold, K. H.; Rheingold, A. L. *Proc. Natl. Acad. Sci. U.S.A.* **2003**, *100*, 3635−3640.
(71) Fulmer, G. R.; Miller, A. J. M.; Sherden, N. H.; Gottlieb, H. E.; Nudelman, A.; Stoltz, B. M.; Bercaw, J. E.; Goldberg, K. I. *Organometallics* **2010**, *29*, 2176−2179.
(72) Takahashi, Y.; Hashimoto, M.; Hikichi, S.; Akita, M.; Moro-oka, Y. *Angew. Chem., Int. Ed.* **1999**, *38*, 3074−3077.
(73) Konnick, M. M.; Guzei, I. A.; Stahl, S. S. *J. Am. Chem. Soc.* **2004**, *126*, 10212−10213.
(74) Wang, W.-D.; Bakac, A.; Espenson, J. H. *Inorg. Chem.* **1995**, *34*, 4049−4056.
(75) Bakac, A.; Wang, W.-D. *J. Am. Chem. Soc.* **1996**, *118*, 10325−10326.
(76) Li, F.; Meier, K. K.; Cranswick, M. A.; Chakrabarti, M.; Van Heuvelen, K. M.; Münck, E.; Que, L., Jr. *J. Am. Chem. Soc.* **2011**, *133*, 7256−7259.